

# Relaxation by clustered ferritin: a model for ferritin-induced relaxation *in vivo*

Yves Gossuin,<sup>1\*</sup> Pierre Gillis,<sup>1</sup> Robert N. Muller<sup>2</sup> and Aline Hocq<sup>1</sup>

<sup>1</sup>Biological Physics Department, University of Mons-Hainaut, 7000 Mons, Belgium

<sup>2</sup>NMR and Molecular Imaging Laboratory, Department of General, Organic and Biomedical Chemistry, University of Mons-Hainaut, 7000 Mons, Belgium

Received 29 June 2006; Revised 13 November 2006; Accepted 28 November 2006

**ABSTRACT:** Ferritin, the iron-storing protein of mammals, is known to darken  $T_2$ -weighted MR images. This darkening could be used for the non-invasive measurement of an organ's iron content. Unexplained discrepancies exist between  $T_2$  data obtained in ferritin-containing tissues and aqueous solutions of ferritin. The clustering of the protein induced by trypsin is used to evaluate the effect of ferritin agglomeration on the relaxation rates. Although the longitudinal relaxation is not significantly influenced by clustering,  $T_2$  depends greatly on the stage of agglomeration: the transverse relaxation rate is higher for a clustered sample than for an unclustered sample. Moreover, the field and inter-echo time dependences of the relaxation rate indicate that the relaxation mechanism may be different between small clusters – where a linear dependence of  $1/T_2$  on  $B_0$  is observed – and large clusters – where a quadratic dependence is observed. These results help to explain the relaxation induced by ferritin in tissues. Copyright © 2007 John Wiley & Sons, Ltd.

**KEYWORDS:** ferritin; clustering; transverse relaxation; iron content of tissues

## INTRODUCTION

Ferritin, the mammalian iron-storage protein, contains a superparamagnetic ferrihydrite ( $5\text{Fe}_2\text{O}_3 \cdot 9\text{H}_2\text{O}$ ) crystal (1,2) which accelerates the transverse NMR relaxation of water.  $T_2$ -weighted MRI was proposed early on for the non-invasive quantification of ferritin-bound iron in the organs. Different MRI protocols have since been elaborated to study the distribution of ferritin in the liver (3–11) and in the brain, especially the extrapyramidal nuclei (12–19).

Simultaneously, different groups have worked on the relaxation of aqueous solutions of horse spleen ferritin and hydrated iron oxide nanoparticles (20–27), in order to provide an understanding of the MRI contrast caused by ferritin. It was first believed that the relaxation induced by ferritin was provoked by the diffusion of water molecules near the magnetic crystal contained inside ferritin. This explanation, known as the outer sphere mechanism, proved to be in contradiction to the experimental relaxation results. Among other things, the unique proportionality between  $1/T_2$  and the applied magnetic field observed in solution (21,22,24) and in tissues (23,28–30) does not match the quadratic dependence

predicted by the outer sphere theory. It was finally shown that ferritin-induced  $T_2$  shortening arises from the binding of water protons to the surface of the ferrihydrite crystal, and an appropriate theoretical model, the proton exchange dephasing model, was subsequently developed (26). This model qualitatively and quantitatively matches the results obtained for aqueous ferritin solutions but does not seem to be sufficient to explain the results for ferritin-containing tissues.

It should be noted that the effect of ferritin on *in vivo* MRI contrast increases with the increase in the imaging magnetic fields, as does  $1/T_2$ . High fields, up to 3 T, are already used to follow the evolution of iron content in diseased brains. However, the MRI protocols for evaluation of iron content are very sensitive to different parameters (type of organ, iron content, degradation of the tissues, etc.), which complicates their routine use in hospitals (31). This is caused by the significant differences between ferritin-induced relaxation in aqueous solutions and in tissues: for the same iron concentration, at 1 T, the transverse relaxation rate is more than three times higher in tissue than in aqueous horse spleen ferritin solution. Even in tissues, the rate is significantly higher in mouse liver than in spleen (30). The reasons for these differences are not really known, even though the *in vivo* clustering of ferritin in organs, which has been shown to depend on the type of organ (32–34), is thought to affect transverse relaxation properties. A first indication of the influence of clustering

\*Correspondence to: Y. Gossuin, Service de Physique Expérimentale et Biologique, Faculté de Médecine, Université de Mons-Hainaut, 24 Avenue du Champ de Mars, 7000 Mons, Belgium.  
E-mail: Yves.gossuin@umh.ac.be

**Abbreviation used:** TEM, transmission electron microscopy.

was given by Wood *et al.* (27): they noticed a large increase in  $1/T_2$  and a significant effect of inter-echo time for “liposomal ferritin” compared with ferritin in solution.

In this work, the controlled clustering of ferritin by the enzyme trypsin was observed in aqueous solutions, by following a protocol initially developed to produce a synthetic analog of hemosiderin (35,36). The NMR relaxation properties of different samples of clustered ferritin were carefully studied, especially the field dependence of the relaxation times and the influence of the inter-echo time on  $1/T_2$ .

## MATERIALS AND METHODS

### Samples

Horse spleen ferritin (ref. F4503) was obtained from Sigma Chemicals (Bornem, Belgium). The average loading factor (number of iron ions per molecule) of the ferritin sample, as determined by inductively-coupled plasma atomic emission spectroscopy (Jobin Yvon JY70+, Longjumeau, France), was about 1120. The hydrodynamic size of the protein is the size derived from the protein diffusion constant, measured by photon correlation spectroscopy (Brookhaven Instruments BI 160, Holtsville, USA). It was less than 30 nm. Solutions containing different proportions of ferritin and trypsin were prepared with deionized water. Trypsin (obtained from Merck (Brussels, Belgium); ref. 108367, activity 200 FIP-U/G) is an enzyme secreted by the pancreas, which breaks down proteins into shorter chains of amino acids. The protective shell of ferritin is thus partially digested in the presence of trypsin, causing the aggregation of the protein.

Solutions containing different relative amounts of ferritin and trypsin were prepared. These samples were sealed and maintained at 37°C and pH ~ 7 throughout the study, to ensure reproducible clustering conditions. The NMR measurements were made after different durations of time (1–180 h) of action by the enzyme. Some of the samples were not studied because insoluble protein aggregates appeared in the tube, especially when the proportion of trypsin was too large. The hydrodynamic size of the aggregates was measured by photon correlation spectroscopy.

Preliminary studies helped to establish the best conditions for slow and reproducible clustering of ferritin. It was decided to use iron concentrations of 16.6–27.7 mM and a mass fraction of trypsin in the range 0.4–3.6%.

### Electron microscopy

The structure and size of the protein clusters was studied by transmission electron microscopy (TEM; Philips

(Eindhoven, The Netherlands) CM 20 Microscope, USA). A small volume of the sample was vaporized on the TEM carbon-coated copper grids to avoid artificial aggregation of the particles during drying of the sample.

### NMR measurements

Relaxation time measurements were performed on Bruker PC120, PC140 and mq 60 instruments operating at magnetic fields ( $B_0$ ) of 0.47, 0.94, and 1.41 T, respectively. A Bruker AMX 300 (7 T) spectrometer was used for the high-field measurements.  $T_2$  was obtained at 37°C with a Carr Purcell Meiboom Gill sequence, with an inter-echo time of 1 ms. The repetition time was always longer than 5  $T_1$ . The monoexponential fits were good, thereby providing no evidence of multiexponential behavior.  $T_1$  NMR dispersion profiles were recorded at 37°C from 0.00023 to 0.23 T on a Spinmaster fast field cycling relaxometer (Stelar, Mede, Italy). The error of the relaxation times was less than 4%. The contribution of trypsin to the relaxation rates of our solutions was shown to be negligible.

## RESULTS

### Clustering protocol

After the addition of trypsin, the size of the clusters changed from less than 30 nm for the initial protein to up to 1400 nm. Above this size, the clusters were too large to stay in solution, and sedimentation was observed. A typical example of the evolution of the cluster size over time is shown in Fig. 1 for the largest concentration in trypsin. It should be noted that clusters with the same size (as in Fig. 1) could be characterized by different inter-crystal distances within the cluster, precisely because trypsin digests the ferritin protein shell. Moreover, sizes obtained by photon correlation spectroscopy are only estimates, because the accuracy of this method is strongly dependent on the size distribution range. To obtain more information about the system, TEM pictures were recorded; the clusters of various size are clearly present (Fig. 2a). Inside an aggregate, the distance between the iron cores is quite small, as observed in TEM images of ferritin-containing tissues (Fig. 2b). TEM results also show that the size distribution of the particles is very broad, and it was therefore not possible to draw an accurate size histogram using TEM images.

### Relaxometry

Figure 3 shows the typical evolution of the relaxation rates at 1.41 T during the clustering process for a 16.6 mM [Fe] ferritin solution containing 3.6% trypsin.  $1/T_1$  first

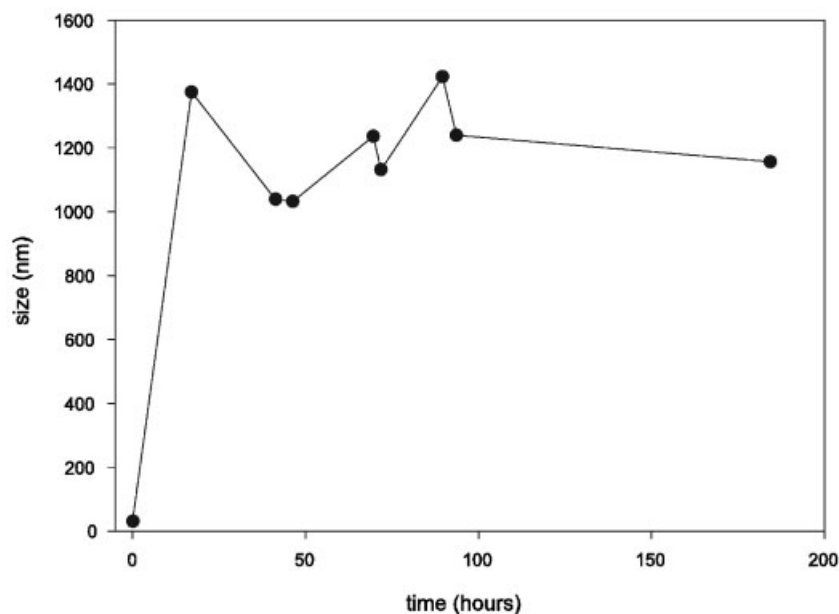


**Figure 1.** Typical evolution of the cluster size during the action of trypsin in a ferritin solution of 16.6 mM [Fe] containing 3.6% trypsin.

decreases and then increases, with significant variation. On the other hand, 180 h after enzymatic digestion,  $1/T_2$  had increased by a factor of 7. However, the samples obtained with this high concentration of trypsin were not perfectly stable in solution, and therefore for the complete relaxometric study, samples with lower concentrations of trypsin were used.

Ferritin solutions containing different amounts of trypsin (0.4%, 0.8%, 1.3%, 1.7%), corresponding to different stages of clustering, were prepared, and the evolution of the relaxation rates according to the magnetic field was measured after 72 h of trypsin action. The corresponding sizes of the ferritin clusters were 140 nm, 860 nm, 890 nm and 840 nm respectively. The  $1/T_1$  vs field curve is not strongly influenced by the clustering of the protein (Fig. 4a). Conversely, the field dependence of  $1/T_2$  with the field is completely different between homogeneous ferritin and clustered ferritin (Fig. 4b). For the unclustered sample,  $1/T_2$  increases linearly with field strength. For the sample with 0.4% trypsin, it remains linear, but the slope of the relationship is increased by a factor of 2. These curves were fitted according to:

$$\frac{1}{T_2} = c_1 B_0 + c_0 \quad (1)$$

For the higher proportions of trypsin,  $1/T_2$  depends quadratically on the magnetic field. The data were fitted according to eqn (2):

$$\frac{1}{T_2} = c_2 B_0^2 + c_1 B_0 + c_0 \quad (2)$$

The derived constants  $c_0$ ,  $c_1$  and  $c_2$  are provided in Table 1.

The effect of the inter-echo time on the transverse relaxation rate was evaluated at 1.41 T and 7 T. This was found to be negligible for the sample with 0.4% trypsin, but was significant for the sample with 1.7% trypsin (Fig. 5). This type of dependence was also observed by Wood *et al.* (27) at 1.41 T for liposomal ferritin.

## DISCUSSION

The size of the ferritin clusters produced by trypsin digestion covers the same range as the clusters observed in human tissues. Indeed, recent TEM studies of ferritin and/or hemosiderin aggregates in human liver (37), human brain (38), and rat liver (39) show that the cluster size is 0.1–1.5  $\mu\text{m}$ , while our clusters have a mean hydrodynamic size of 1  $\mu\text{m}$ .

In contrast with previous studies on liver samples, the decay of transverse magnetization of our samples was monoexponential. For iron-loaded tissues at high field, biexponential (28) or non-exponential behaviors (37,40) were observed. This difference could be explained by compartmentalization of water in tissues, which does not occur in solutions. However, Ghugre *et al.* (37) suggest that this compartmentalization is due to magnetic susceptibility effects rather than to anatomical divisions. If they are right, this effect would be observed even in solution, but for higher iron concentrations than in our samples. However, for brain tissues, the relaxation induced by ferritin is monoexponential (23,29).

The effect of clustering on longitudinal relaxation (Fig. 3) is far from simple, with first a decrease and then an increase in  $1/T_1$ . A satisfactory explanation for this behavior is difficult to find, as, even for unclustered

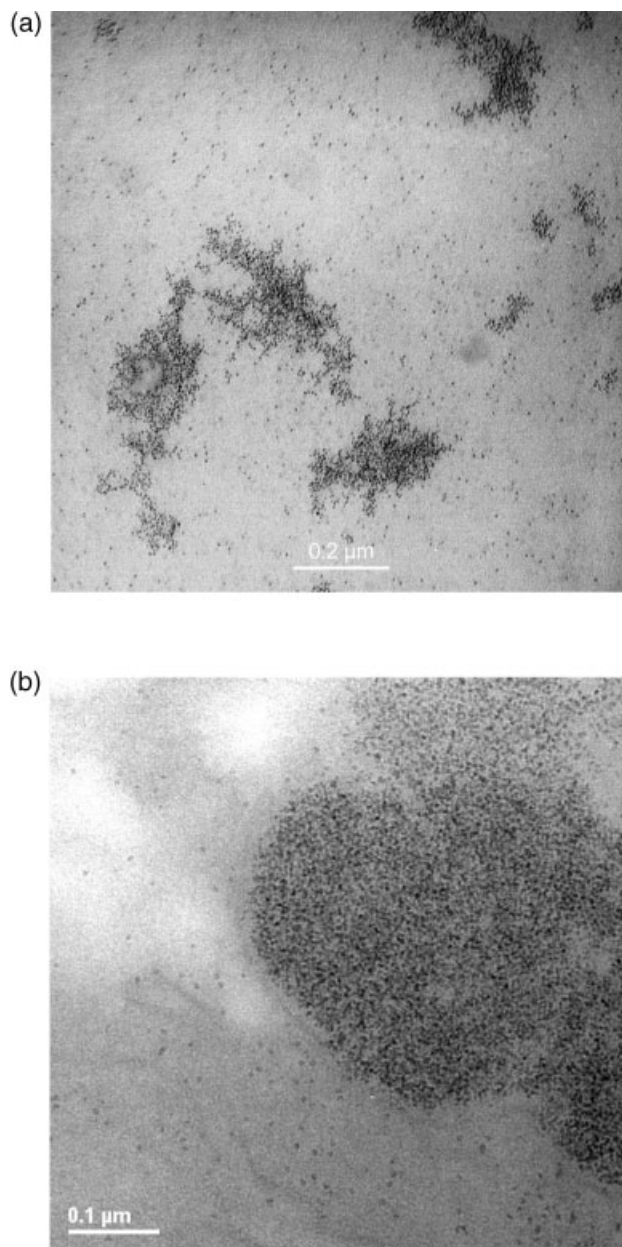


**Figure 2.** TEM pictures of (a) clusters of ferritin obtained in a 27.7 mM [Fe] ferritin solution containing 1.7% trypsin after 50h and (b) clusters of ferritin observed *in vivo* [from reference (34)].

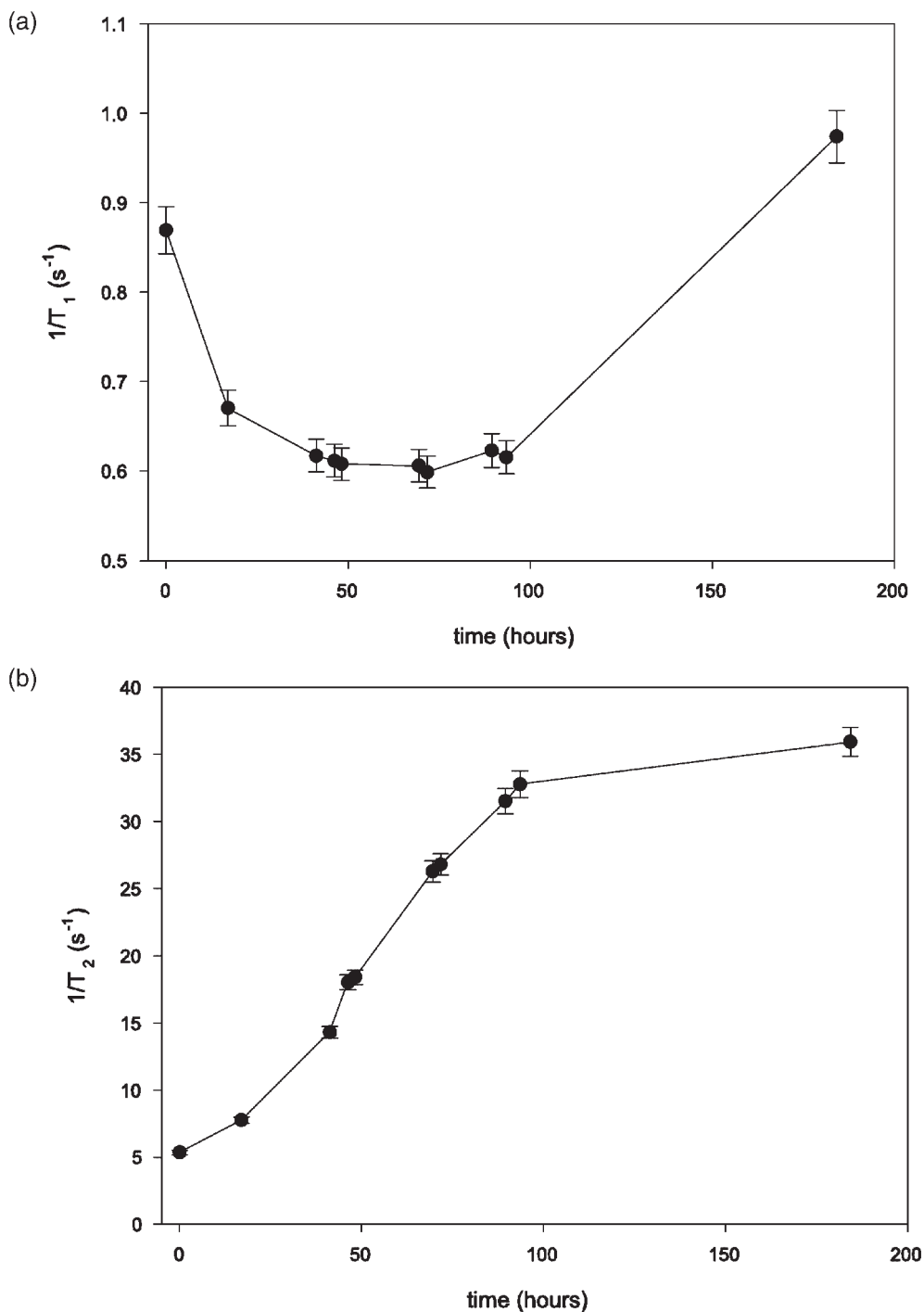
ferritin solution, the longitudinal relaxation mechanism is not completely understood. However, the agglomeration process must modify important correlation times, such as the Néel relaxation time of the ferrihydrite crystals, the diffusion time of water protons around the clusters, and the cluster rotation time. These three parameters play a crucial role in longitudinal relaxation.

The least expected aspect of the NMR relaxation behavior of ferritin in the past has always been the linearity of  $1/T_2$  with  $B_0$ . Indeed, the prediction of the outer sphere model, proposed early on for ferritin (20,21), was a quadratic dependence of the rate. From different

studies, it appeared that this linearity was associated with a proton exchange process between bulk water and the surface of the ferrihydrite crystal. With this study, a quadratic dependence of  $1/T_2$  with  $B_0$  is observed experimentally for the first time, even if one suspects that the liposomal ferritin sample synthesized by Wood *et al.* (27) presents the same field dependence. Beyond a certain stage of clustering, “quadratic” relaxation dominates, whereas for unclustered or slightly clustered samples, it is “linear” relaxation that dominates. These different NMR behaviors cannot be explained by changes in magnetic properties of the sample, which were unaltered by clustering, as checked by vibrating sample magnetometry.

For the unclustered ferritin solution, the slope of the linear dependence between  $1/T_2$  and  $B_0$  is consistent with previous results (21,24). The slope obtained for the sample with 0.4% trypsin is close to that obtained for ferritin-containing brain tissue (Table 1). Table 2 shows the transverse relaxivities  $r_2$  ( $1/T_2$  values normalized per unit iron concentration) at 1.41 T for our different samples and for the liposomal ferritin sample of reference (30). The relaxivity clearly increases with trypsin concentration but remains below that of liposomal ferritin. Of course, the two systems are quite different: a sphere of aggregated ferritin molecules for our samples and a liposome with its surface covered with ferritin molecules for the sample of Wood *et al.* For the sample with 1.7% trypsin, the relaxivity obtained at 7 T is the highest ever observed for a ferritin sample. In comparison with the unclustered sample, the relaxation rate has increased by a factor of 5. Moreover, for this sample, the field dependence is clearly quadratic. It would be interesting to check if, for iron-overloaded tissues,  $r_2$  increases quadratically at high fields. This may be of interest for the non-invasive detection of ferritin-bound iron by high-field MRI. However, the accurate quantification of ferritin iron may become more complex, because of the dependence of the relaxation rates on clustering, which also occurs *in vivo*. It is thus possible that, for some tissues, the field-dependent rate-increase method (16), based on the assumption that  $1/T_2$  increases linearly with the field, is no longer valid.

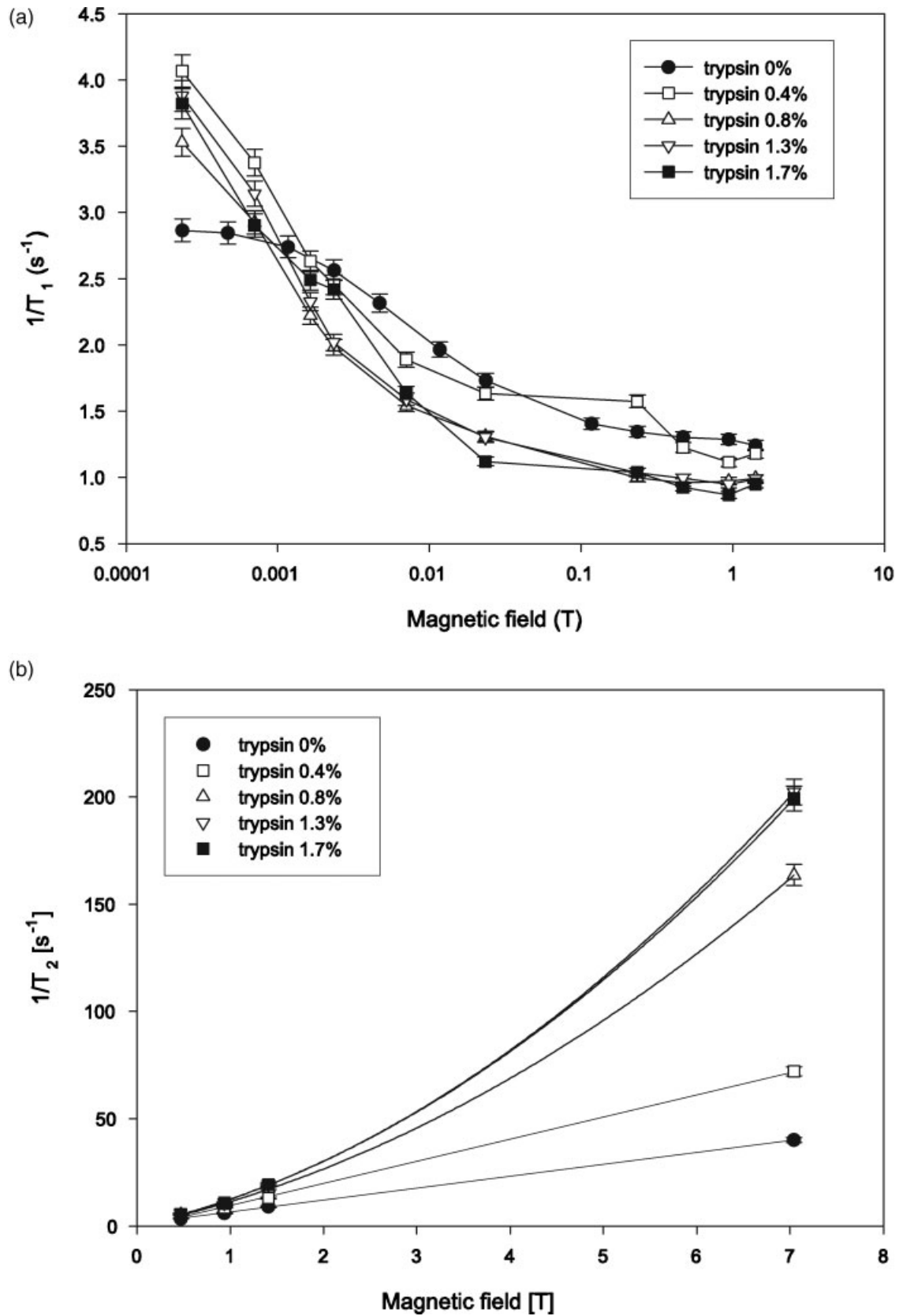
The theoretical explanation for the results reported here is not straightforward: it seems that multiple relaxation mechanisms coexist. The relative importance of these mechanisms must vary depending on different parameters (magnetic field, size of the clusters, shape of the clusters). The first mechanism is the proton exchange already described for aqueous solutions of ferritin, with a linear dependence of  $1/T_2$  on  $B_0$  and no influence of the inter-echo time on transverse relaxation. The second mechanism may be diffusion around the clusters; this type of relaxation regime depends on the value of  $\Delta\omega\tau_D$ , where  $\tau_D = \frac{R^2}{D}$  is the diffusion correlation time and  $\Delta\omega = \gamma \frac{\mu_0\mu}{R^3}$  is the angular frequency shift experienced by a proton at the equatorial line of the cluster surface (20). For the



**Figure 3.** Evolution of (a)  $1/T_1$  and (b)  $1/T_2$  of a 16.6 mM [Fe] ferritin solution containing 3.6% trypsin with the time of clustering at 1.41 T.

ferritin solution containing 1.7% trypsin at 1 T,  $R=420$  nm and  $\mu=1.04 \times 10^{-22}$  Am<sup>2</sup>. Taking  $D=3 \times 10^{-9}$  m/s<sup>2</sup>, one obtains  $\Delta\omega\tau_D \approx 4$ , which means that this contribution is not typical outer sphere relaxation, but rather an intermediate regime between outer sphere and the static dephasing regime (41). A third mechanism may be the diffusion of water molecules

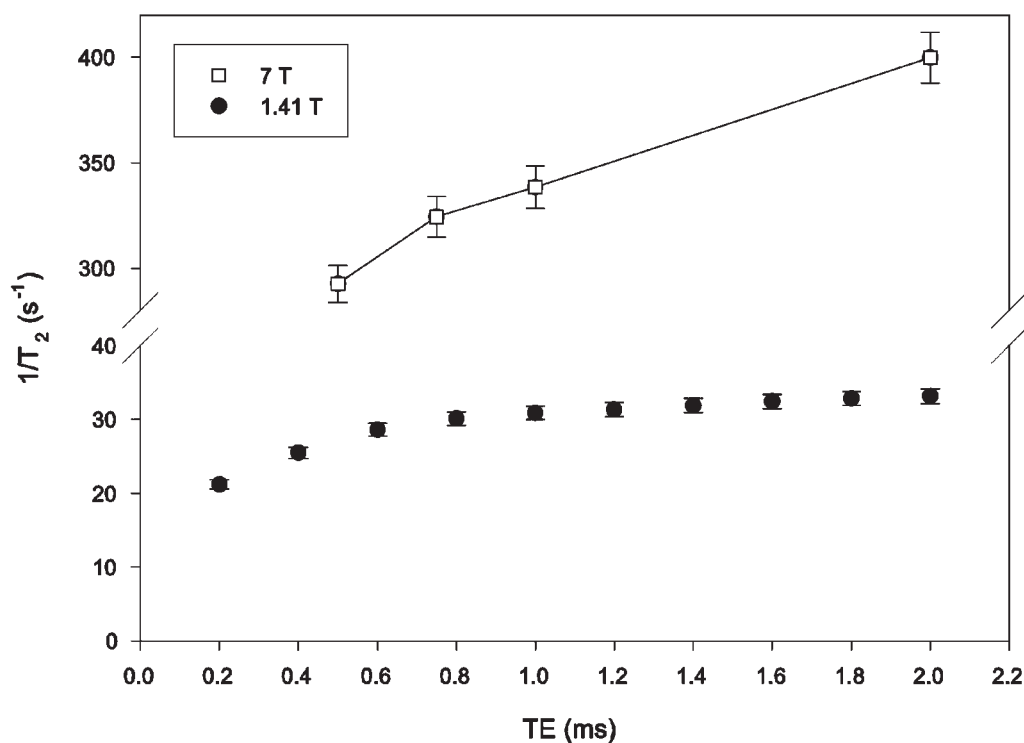
inside the clusters, within smaller-scale field homogeneities. For larger aggregates, the dominating relaxation mechanism should be the static dephasing regime, with a large influence of the inter-echo time on transverse relaxation. However, larger clusters were not stable in aqueous solutions and our samples thus had a maximum size of 1000 nm.



**Figure 4.** Evolution of (a)  $1/T_1$  and (b)  $1/T_2$  with magnetic field for a 27.7 mM [Fe] ferritin solution containing 0.4%, 0.8%, 1.4% and 1.7% trypsin after 72 h.

**Table 1. Parameters of the fitting of the  $1/T_2$  versus field curves.  $[Fe] = 27.7$  mM**

Sample	$c_0$ ( $s^{-1}$ )	$c_1$ ( $s^{-1}T^{-1}$ )	$c_2$ ( $s^{-1}T^{-2}$ )
0% trypsin (unclustered ferritin)	0.94	5.54	—
0.4% trypsin	-0.65	10.3	—
0.8% trypsin	0.22	9.24	1.98
1.3% trypsin	0.32	9.54	2.72
1.7% trypsin	-0.10	9.95	2.61
Ferritin in globus pallidus (23) (normalized to 27.7 mM)	—	9.46	—

**Figure 5.** Evolution of  $1/T_2$  with the inter-echo time at 60 MHz and 300 MHz for a 27.7 mM  $[Fe]$  ferritin solution containing 1.7% trypsin.**Table 2. Values of  $r_2$  for ferritin solutions containing different amounts of trypsin, after 72 h at 1.41 T**

Sample	$r_2$ ( $s^{-1}mM^{-1}$ )
0% trypsin (unclustered ferritin)	0.324
0.4% trypsin	0.470
0.8% trypsin	0.637
1.3% trypsin	0.708
1.7% trypsin	0.700
Liposomal ferritin (27)	1.428

The size of the clusters does not seem to be the only crucial parameter determining transverse relaxation: Figs 1 and 3b show that even when the size is almost constant, the transverse relaxation rate keeps increasing, probably because the inter-crystal distance inside a cluster decreases during the action of trypsin, which causes an increase in the clusters' magnetization.

The results of this study, i.e. the effect of clustering on the relaxation induced by ferritin, make it possible to explain the different NMR behavior observed for ferritin solutions and ferritin-containing tissues. They also help us to understand why, for the same iron concentration, different organs exhibit different  $T_2$  values. The influence of clustering on transverse relaxation is at the same time an opportunity for the qualitative detection of iron overload by MRI (because of the observed increase in transverse relaxivity) and also a problem for the accurate determination of iron content, because the relaxation rate depends on the iron content *and* on the stage of clustering.

## REFERENCES

- Harrison PM, Arosio P. The ferritins: molecular properties, iron storage function and cellular regulation. *Biochim. Biophys. Acta* 1996; **1275**: 161–203.

2. Cornell RM, Schwertmann U. *The Iron Oxides*. VCH: Weinheim, 1996.
3. Stark DD, Bass NM, Moss AA, Bacon BR, McKerrow JH, Cann CE, Brito A, Goldberg HI. Nuclear magnetic resonance imaging of experimentally induced liver disease. *Radiology* 1983; **148**: 743–751.
4. Engelhardt R, Langkowski JH, Fischer R, Nielsen P, Kooijman H, Heinrich HC, Bücheler E. Liver iron quantification: studies in aqueous iron solutions, iron overloaded rats, and patients with hereditary hemochromatosis. *Magn. Reson. Imaging* 1994; **12**: 999–1007.
5. Gomori JM, Horev G, Tamary H, Zandback J, Kornreich L, Zaizov R, Freud E, Krief O, Ben-Meir J, Rotem H, Kuspet M, Rosen P, Rachmilewitz EA, Loewenthal E, Gorodetsky R. Hepatic iron overload: quantitative MR imaging. *Radiology* 1991; **179**: 367–369.
6. Papakonstantinou OG, Maris TG, Kostaridou V, Gouliamos AD, Koutoulas GK, Kalovidouris AE, Papavassiliou GB, Kordas G, Kattamis C, Vlahos LJ, Papavassiliou CG. Assessment of liver iron overload by T<sub>2</sub>-quantitative magnetic resonance imaging: correlation of T<sub>2</sub>-QMRI measurements with serum ferritin concentration and histologic grading of siderosis. *Magn. Reson. Imaging* 1995; **13**: 967–977.
7. Fenzi A, Bortolazzi M, Marzola P, Colombari R. *In vivo* investigation of hepatic iron overload in rats using T2 maps: quantification at high intensity field (4.7-T). *J. Magn. Reson. Imaging* 2001; **13**: 392–396.
8. Stark DD, Moseley ME, Bacon BR, Moss AA, Goldberg HI, Bass NM, James TL. Magnetic resonance imaging and spectroscopy of hepatic iron overload. *Radiology* 1985; **154**: 137–142.
9. Clark PR, Chua-Anusorn W, St Pierre TG. Proton transverse relaxation rate (R<sub>2</sub>) images of iron-loaded liver tissue: mapping local tissue iron concentrations with MRI. *Magn. Reson. Med.* 2003; **49**: 572–575.
10. St Pierre TG, Clark PR, Chua-Anusorn W. Single spin-echo proton transverse relaxometry of iron-loaded liver. *NMR Biomed.* 2004; **17**: 446–458.
11. Bonkovsky HL, Rubin RB, Cable EE, Davidoff A, Rijcken THP, Stark DD. Hepatic iron concentration: Noninvasive estimation by means of MR imaging techniques. *Radiology* 1999; **212**: 227–234.
12. Drayer B, Burger P, Darwin R, Riederer S, Herfkens R, Johnson GA. Magnetic resonance imaging of brain iron. *AJR Am. J. Roentgenol.* 1986; **147**: 103–110.
13. Schenck JF. Imaging of brain iron by magnetic resonance: T<sub>2</sub> relaxation at different field strengths. *J. Neurol. Sci.* 1995; **134S**: 10–18.
14. Gelman N, Gorell JM, Barker PB, Savage RM, Spickler EM, Windham JP, Knight RA. MR imaging of human brain at 3.0 T: preliminary report on transverse relaxation rates and relation to estimated iron content. *Radiology* 1999; **210**: 759–767.
15. Ordidge RJ, Gorell JM, Deniau JC, Knight RA, Helpert JA. Assessment of relative brain iron concentrations using T<sub>2</sub>-weighted and T<sub>2</sub>\*-weighted MRI at 3 Tesla. *Magn. Reson. Med.* 1994; **32**: 335–341.
16. Bartzokis G, Aravagiri M, Oldendorf WH, Mintz J, Marder SR. Field dependent transverse relaxation rate increase may be a specific measure of tissue iron stores. *Magn. Reson. Med.* 1993; **29**: 459–464.
17. Ye FQ, Martin WR, Allen PS. Estimation of brain iron *in vivo* by means of the interecho time dependence of image contrast. *Magn. Reson. Med.* 1996; **36**: 153–158.
18. Schenck JF, Zimmerman EA. High-field magnetic resonance imaging of brain iron: birth of a biomarker? *NMR in Biomed.* 2004; **17**: 433–445.
19. Haacke EM, Cheng NYC, House MJ, Liu Q, Neelavalli J, Ogg RJ, Khan A, Ayaz M, Kirsch W, Obenaus A. Imaging iron stores in the brain using magnetic resonance imaging. *Magn. Reson. Imaging* 2005; **23**: 1–25.
20. Gillis P, Koenig SH. Transverse relaxation of solvent protons induced by magnetized spheres: application to ferritin, erythrocytes, and magnetite. *Magn. Reson. Med.* 1987; **5**: 323–345.
21. Vymazal J, Brooks RA, Zak O, McRill C, Shen C, Di Chiro G. T<sub>1</sub> and T<sub>2</sub> of ferritin at different field strengths: effect on MRI. *Magn. Reson. Med.* 1992; **27**: 368–374.
22. Bulte JW, Vymazal J, Brooks RA, Pierpaoli C, Frank JA. Frequency dependence of MR relaxation times. II. Iron oxides. *J. Magn. Reson. Imaging* 1993; **3**: 641–648.
23. Brooks RA, Vymazal J, Bulte JWM, Baumgarner CD, Tran V. Comparison of T2 relaxation in blood, ferritin, and brain. *J. Magn. Reson. Imaging* 1995; **5**: 446–450.
24. Gossuin Y, Roch A, Muller RN, Gillis P. Relaxation induced by ferritin and ferritin-like magnetic particles: the role of proton exchange. *Magn. Reson. Med.* 2000; **43**: 237–243.
25. Gossuin Y, Roch A, Lo Bue F, Muller RN, Gillis P. Nuclear magnetic relaxation dispersion of ferritin and ferritin-like magnetic particle solutions: a pH-effect study. *Magn. Reson. Med.* 2001; **46**: 476–481.
26. Gossuin Y, Roch A, Muller RN, Gillis P, Lo Bue F. Anomalous nuclear magnetic relaxation of aqueous solutions of ferritin : an unprecedented first-order mechanism. *Magn. Reson. Med.* 2002; **48**: 959–964.
27. Wood JC, Fassler JD, Meade T. Mimicking liver iron overload using liposomal ferritin preparations. *Magn. Reson. Med.* 2004; **51**: 607–611.
28. Bulte JWM, Miller GF, Vymazal J, Brooks RA, Frank JA. Hepatic hemosiderosis in non-human primates: quantification of liver iron using different field strengths. *Magn. Reson. Med.* 1997; **37**: 530–536.
29. Vymazal J, Brooks RA, Baumgarner C, Tran V, Katz D, Bulte JW, Bauminger R, Di Chiro G. The relation between brain iron and NMR relaxation times: an *in vitro* study. *Magn. Reson. Med.* 1996; **35**: 56–61.
30. Gossuin Y, Burtea C, Monseux A, Toubeau G, Roch A, Muller RN, Gillis P. Ferritin-induced relaxation in tissues: an *in vitro* study. *J. Magn. Reson. Imaging* 2004; **20**: 690–696.
31. Brittenham GM, Badman DG. Noninvasive measurement of iron: report of an NIDDK workshop. *Blood* 2003; **101**: 15–19.
32. Richter GW. The cellular transformation of injected colloidal iron complexes into ferritin and hemosiderin in experimental animals. *J. Exp. Med.* 1959; **109**: 197–214.
33. Smith AG, Carthew P, Francis JE, Edwards RE, Dinsdale D. Characterization and accumulation of ferritin in hepatocyte nuclei of mice with iron overload. *Hepatology* 1990; **12**: 1399–1405.
34. Brown A, Brydson R, Calvert CC, Warley A, Bomford A, Li A, Powell J. *Analytical electron microscope investigation of iron within human liver biopsies. Electron Microscopy and Analysis Conference* 2003; Oxford.
35. Wixom RL, Prutkin L, Munro HN. Hemosiderin: nature, formation and significance. *Int. Rev. Exp. Pathol.* 1980; **22**: 193–225.
36. Matioli GT, Baker RF. Denaturation of ferritin and its relationship with hemosiderin. *J. Ultrastruct. Res.* 1963; **8**: 477–490.
37. Ghugre NR, Coates TD, Nelson MD, Wood JC. Mechanisms of tissue-iron relaxivity: nuclear magnetic resonance studies of human liver biopsy specimens. *Magn. Reson. Med.* 2005; **54**: 1185–1193.
38. Quintana C, Bellefqih S, Laval JY, Guerin-Kern JL, Wu TD, Avila J, Ferrer I, Arranz R, Patino C. Study of the localization of iron, ferritin, and hemosiderin in Alzheimer's disease hippocampus by analytical microscopy at the subcellular level. *J. Struct. Biol.* 2005; **153**: 42–51.
39. Gutierrez L, Lazaro FJ, Abadia AR, Romero MS, Quintana C, Puerto Morales M, Patino C, Arranz R. Bioinorganic transformations of liver iron deposits observed by tissue magnetic characterization in a rat model. *J. Inorg. Biochem.* 2006; **100**: 1790–1799.
40. Jensen JH, Chandra R. Theory of nonexponential NMR signal decay in liver with iron overload or superparamagnetic iron oxide particles. *Magn. Reson. Med.* 2002; **47**: 1131–1138.
41. Roch A, Gossuin Y, Muller RN, Gillis P. Superparamagnetic colloid suspensions: water magnetic relaxation and clustering. *Journal of Magnetism and Magnetic Materials* 2005; **293**: 532–539.